PCCP

Are All Charge-Transfer Parameters Created Equally? A Study of Functional Dependence and Excited-State Charge-Transfer Quantification Across Two Dye Families

Journal:	*Physical Chemistry Chemical Physics*
Manuscript ID	CP-ART-07-2021-003383.R1
Article Type:	Paper
Date Submitted by the Author:	24-Aug-2021
Complete List of Authors:	Marshburn, Richard; North Carolina State University, Chemistry Ashley, Daniel; North Carolina State University, Chemistry Curtin, Gregory; North Carolina State University, Chemistry Sultana, Nadia; NC State University, College of Textiles Liu, Chang; North Carolina State University, Chemistry Vinueza, Nelson; North Carolina State University, Textile Engineering, Chemistry and Science Ison, Elon; North Carolina State University, Chemistry Jakubikova, Elena; North Carolina State University, Chemistry

Are All Charge-Transfer Parameters Created Equally? A Study of Functional Dependence and Excited-State Charge-Transfer Quantification Across Two Dye Families

Richard Drew Marshburn,[†,¶] Daniel C. Ashley,[†,¶] Gregory M. Curtin,[†] Nadia Sultana,[‡] Chang Liu,[†] Nelson R. Vinueza,[‡] Elon A. Ison,[†] Elena Jakubikova[†]*

[†]Department of Chemistry, North Carolina State University, Raleigh, North Carolina 27695, United States

[‡]Department of Textile Engineering, Chemistry, and Science, North Carolina State University, 1020 Main Campus Drive, Raleigh, NC 27606, United States

[¶]Contributed equally to this work.

ABSTRACT:

Small molecule organic dyes have many potential uses in medicine, textiles, forensics, and light-harvesting technology. Being able to computationally predict the spectroscopic properties of these dyes could greatly expedite screening efforts, saving time and materials. Time-dependent density functional theory (TD-DFT) has been shown to be a good tool for this in many instances, but characterizing electronic excitations with charge-transfer (CT) character has historically been challenging and can be highly sensitive to the chosen exchange-correlation functional. Here we present a combined experimental and computational study of the excited-state electronic structure of twenty organic dyes obtained from the Max Weaver Dye Library at NCSU. Results of UV-Vis spectra calculations on these dyes with six different exchange-correlation functionals: BP86, B3LYP, PBE0, M06, BHandHLYP, and CAM-B3LYP were compared against their measured UV-Vis spectra. It was found that hybrid functionals with modest amounts (20-30%) of included Hartree-Fock exchange are the most effective at matching the experimentally determined λ_{max}. The interplay between the observed error, the functional chosen, and the degree of CT was analyzed by quantifying the CT character of λ_{max} using four orbital and density-based metrics, Λ, Δr, S_C and D_{CT}, as well as the change in the dipole moment, $\Delta\mu$. The results showed that the relationship between CT character and the functional dependence of error is not straightforward, with the observed behavior being dependent both on how CT was quantified and the functional groups present in the molecules themselves. It is concluded that this may be a result of the examined excitations having intermediate CT character. Ultimately it was found that the nature of the molecular "family" influenced how a given functional behaved as a function of CT character, with only two of the examined CT quantification methods, Δr and D_{CT}, showing consistent behavior between the different molecular families. This suggests that further work needs to be done to ensure that currently used CT quantification methods show the same general trends across large sets of multiple dye families.

Introduction

Throughout human history, dyes have held an important place in our shared cultural and technological landscape.[1] For example, in the distant past dyes such as Tyrian purple, produced from crushed invertebrates, were heavily traded by the Phoenicians which led to purple becoming a significant cultural symbol for wealth, royalty, and even divinity.[1] The great variety of dyes and our detailed characterizations of their properties have made dye science a vital tool in present-day forensics,[2] with unique dye characteristics being traceable to fiber evidence obtained from a crime scene. With the advent of modern printing, the textile industry, photodynamic cancer therapy, and ecologically conscious production processes, the demand for affordable non-toxic dyes with specifically tailored properties has steadily increased within the last two centuries. This has led to the effective synthesis and experimental characterization of numerous organic dyes. One large, relatively untapped resource of dyes is the Max Weaver Dye Library (MWDL) located at North Carolina State University (NCSU).[3] The MWDL, generously donated by Eastman Chemical Company to NCSU, contains upwards of 90,000 dyes that could potentially satisfy the requirements of industries across many disciplines. A drawback to the massive size of the MWDL is that many of these compounds are only minimally characterized beyond basic structural information, creating problems for researchers that wish to obtain dyes with specific properties. Measuring the optical properties of each and every dye would be an enormous and costly undertaking.

A potential solution to this dilemma is to use modern electronic structure theory to computationally evaluate the spectral behavior of the synthesized dyes. While many *ab initio* wavefunction-based methods are capable of predicting the UV-Vis spectra of small to medium organic compounds with high accuracy,[4] their considerable computational cost makes them impractical for screening such a large number of molecules.[5] Fortunately, density functional theory (DFT)[6] and time-dependent DFT (TD-DFT)[7-8] provide an optimal balance between efficiency and accuracy and are an excellent means for studying the photochemical properties of small organic compounds.[5, 9-10] Unfortunately, the accuracy of the results obtained from TD-DFT calculations often strongly depends on the chosen density functional and this continually leads to the basic question: which methodology should researchers choose to most effectively match or predict experimental results? Aside from resolving this practical question, a study of these functionals may also help determine *why* one functional is more effective than another, which could aid in the

development of more accurate functionals. Thus, DFT and the MWDL form a symbiotic relationship: DFT being a useful tool for characterizing the MWDL, while the MWDL provides experimental data for DFT benchmarking and methodology optimization.

In this work, we make use of the MWDL to provide a small but reasonable test set of interesting compounds from two dye families: dyes containing an azobenzene[11-12] moiety (hereafter referred to as "azo dyes") and dyes containing a cyanovinyl[13] group (hereafter referred to as "cyano dyes"), see Figure 1. The UV-Vis spectra of these dyes were measured experimentally after being taken directly from the MWDL. The spectra were then also calculated using a variety of TD-DFT methods, enabling us to determine what functional is the most accurate.

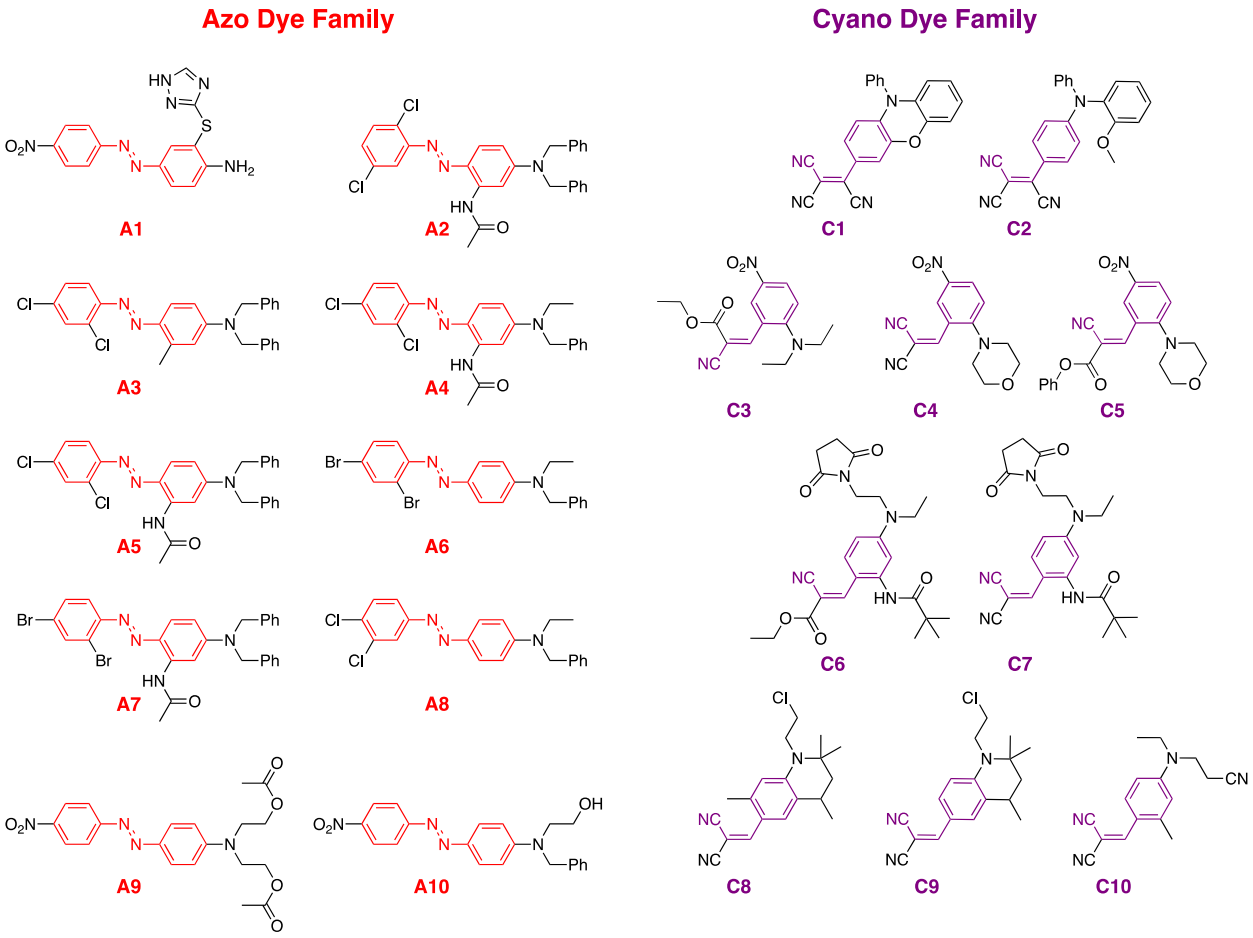

Figure 1. Dyes examined in this study, grouped by their respective families. The parent dyes are highlighted in red and purple.

When discussing the performance of DFT functionals, it has been shown that both the functional dependence and TD-DFT accuracy can often be related back to the nature of the excited states being investigated.[10, 14] These states can be broadly categorized as local (valence and

Rydberg) excitations and charge transfer (CT) excitations. Careful determination of the CT character of a transition can potentially assist in predicting what type of functional should be used.[14-21] The amount of Hartree-Fock exchange (HF_{Ex}) included in the functional has emerged as an important tunable parameter for calibrating a DFT methodology. A typical conclusion reached from these studies is that functionals with high amounts of HF_{Ex} show less sensitivity to the CT character of a transition when trying to match experiment.[14] Specifically, range-separated functionals (low HF_{Ex} at short distances and high HF_{Ex} at large distances) and functionals with high HF_{Ex} in general,[22] have been indicated as being highly effective for characterizing transitions with high CT character.[10, 14, 21, 23] It has also been shown that non-empirically optimally-tuned range-separated functionals can perform very well for characterizing electronic excitations, particularly ones with large CT-character.[24-27] Other work has shown that these optimally-tuned functionals can be significantly flawed in other areas however,[28] highlighting the fact that many challenging features have to be overcome simultaneously in the quest to develop truly all-purpose DFT methods. For local valence (referred to simply as "local" here) excitations, however, functionals with modest HF_{Ex} often perform as well as range-separated functionals or functionals with high HF_{Ex}, if not sometimes better.[10, 29-30] Pure GGA functionals almost always perform poorly.[29, 31] Note that accurate computation of Rydberg transitions is also a challenging area for TD-DFT, however, the focus of this study is on lower energy transitions (particularly in the visible or UV regions), which are rarely Rydberg in nature, and hence these issues will not be explored further. Ultimately, while many DFT functionals and methodologies are worth evaluating, for this study we chose to limit our scope to a small set of standard methods, with plans to consider other functional types in the future.

In our test set, we quantified the CT character of the dye excitations in several ways to explore the relationship between CT character and the success of the chosen DFT methods. Specifically, we examined five different CT parameters: Λ, Δr, S_C, D_{CT}, and $\Delta\mu$. Λ and Δr are orbital-based and determine the magnitude of CT by comparing orbital overlap or the spatial distance between orbitals, respectively.[14, 16] On the other hand, S_C and D_{CT} are density-based parameters and characterize the magnitude of CT by comparing excited state density difference overlap or the spatial distance the excited state density has moved, respectively.[15, 32] Finally, $\Delta\mu$ is

based on the change in dipole moment between the excited and ground state, which can be related to D_{CT} by the amount of charge transferred, q_{CT}.[15]

Λ was one of the first parameters developed for quantification of CT character. The initial study with this parameter on a test set of 18 molecules demonstrated that functionals with low-to-moderate HF_{Ex} have errors that depend on CT character.[14] D_{CT} was later developed as a density-based CT parameter and was evaluated on a series of push-pull oligophenylene compounds, along with Δμ.[15] Subsequently, Δr[16] and its variant based on NTOs[17] were created and tested on a modified form of the original Λ benchmark set where numerous other challenging molecules were included. Δr was found to be a good complement to Λ, and it was proposed that the two be considered together to evaluate CT, especially as Δr was found to be superior to Λ in more challenging cases.[16] It has also been shown that the two distance-based methods, Δr and D_{CT}, correlate well with each other when tested on the large "Real-Life Molecules" test set.[33] However, to our knowledge, all three of these CT parameters (Λ, Δr, and D_{CT}) have never been compared simultaneously using the same dataset. Finally, S_C is a particularly interesting parameter, as it was proposed as a CT quantification tool in the Multiwfn software package.[32] While S_C is based on some of the same theory used to define D_{CT}, to our knowledge, it has not been tested on any large-scale datasets in the literature.

The study presented herein represents, to our knowledge, first comparison of all five CT parameters on the same data set. The twenty compounds studied here showed generally modest to small CT character, however, these conclusions are not always the same depending on how the CT is quantified. This provided the opportunity to examine the relationship between CT and method accuracy for transitions that are hard to classify as either CT or local. Importantly, the selected compounds in many ways represent a real-world dataset, as they were chosen essentially randomly from the vast MWDL after verifying they fit into one of the molecular families of interest, and then were experimentally characterized and subjected to computational study. Thus, this study is a "live-fire" test of TD-DFT, CT quantification, and the utility of the MWDL.

We found that despite showing a larger error dependence on CT character, hybrid functionals with modest (20 to 30%) HF_{Ex} are the most reliable for each dye family, significantly outperforming a popular range-separated functional, CAM-B3LYP.[34] We also found that the relationship between error, CT character, and functional dependence is not straightforward for

transitions with only moderate CT character. Notably, the trends are not consistent between each dye family, with only two out of the five CT parameters (Δr and D_{CT}) showing the same general trends with respect to functional dependence for both families consistently. This suggests that there may be molecular structure-specific factors at work that play a role in producing the functional dependence. While these results are only for two dye families, it raises the possibility that none of the current CT parameters will be universally consistent for a broader test set of multiple diverse molecular families. This highlights some of the successes and remaining challenges in characterizing the CT character of excitations and benchmarking DFT methods for a large set of structurally diverse compounds.

Methodology

UV-Vis Measurements and Other Characterization

Samples of each dye were taken directly from the MWDL; no further purification was performed. These complexes were dissolved in acetonitrile and UV-Vis spectra were measured using a Varian Cary 50 spectrophotometer. The dyes were also subjected to characterization by NMR and LC-MS, the results of which are all provided in the Supporting Information.

Computational Methods

Structure optimizations and excited state calculations

All structures were optimized in vacuum with the B3LYP[35-38] functional including Grimme's D2 dispersion correction (B3LYP+D2).[39] The 6-311G* basis set[40] and an ultrafine grid were used for all calculations. Optimizations were performed in the gas phase, and all structures were confirmed to be genuine minima from frequency calculations using the harmonic oscillator approximation. All TD-DFT calculations were performed using the basis set indicated above with the solvent (acetonitrile) modeled with an implicit polarized continuum model (IEFPCM) using nonequlibrium solvation.[41-43] In order to compare the TD-DFT results to the experimental UV-Vis data, the calculated stick spectra were convoluted with the excitation energies times their respective oscillator strength using a Lorentzian function with half-width-at-half-maximum (HWHM) of 0.33 eV.

The solvent polarization was modeled within the standard linear response (LR) framework. Given that it has been reported that CT transitions can be poorly described by the LR scheme,[44] state-specific (SS) solvation was also investigated using the method demonstrated by Improta,

Barone, Scalmani, and Frisch (IBSF).[45] These results are discussed briefly at the end of the paper, but unless noted otherwise all data is calculated using the LR polarization scheme.

Several functionals were employed to conduct TD-DFT calculations on the B3LYP+D2 optimized structures. The functionals chosen were BP86,[35, 46] B3LYP, PBE0,[47-50] M06,[51] BHandHLYP, and CAM-B3LYP.[34] The twenty five lowest-energy excited states were calculated for all dyes with all functionals, with the exception of BP86 where only the five lowest-energy excited states were considered. For BP86, calculations with more than the five lowest-energy excited states failed to converge. However, for B3LYP and M06, the results obtained for the excited states analyzed in this work, which correspond to either the first or second lowest energy excited state, are identical irrespective of whether 5 or 25 states were calculated in the TD-DFT calculations. All electronic structure calculations were performed with the Gaussian 09 software package revision D.01.[52]

Quantification of CT character

Numerous parameters exist for quantifying CT character in electronic excitations and several of these were applied to explore the relationship between CT and functional dependence. These techniques have already been described in great detail in the literature,[14-16] but as they are important for the analysis in this work, a brief overview of each will be provided below. In general, these parameters can be sorted into two categories: orbital-based parameters and density-based parameters.

Orbital-Based Parameters

The two orbital-based parameters used here employ the ground state Kohn-Sham (KS) orbitals, φ_i and φ_a for occupied and unoccupied orbitals, respectively, and the excitation coefficients (K_{ia}) determined for a relevant excitation from TD-DFT. The excited state wavefunction can be described in terms of the linear combinations of pairs of ground state molecular orbitals weighted with K_{ia} (K_{ia} includes both excitation and de-excitation pairs, however the latter only contribute small amounts in the present study). The first orbital-based parameter is the Λ index proposed by Tozer *et al.*, which provides a measurement of the degree of spatial overlap between the orbital pairs involved in constructing the excited state.[14] A completely local excitation will have complete spatial overlap between the φ_{ia} pair, resulting in a Λ value of 1, while an entirely CT excitation will have no overlap, resulting in a Λ value of 0. The Δr index proposed by Adamo *et al.* also makes use of φ_{ia} and K_{ia}, but it measures the distance between the centroids

of each orbital instead of calculating the spatial overlap between the φ_i, φ_a pairs.[16] This provides an MO-based description of how far the electron has "moved" during the excitation. The greater this distance, the greater the CT character.

Density-Based Parameters

Interpreting CT in terms of the molecular orbitals involved is useful from the perspective of traditional electronic structure theory and how to assign transitions. Alternatively, CT can be characterized by changes in the overall electron density of the molecule during an excitation. The change in electronic structure during an electronic transition can be expressed as the density difference, $\Delta\rho(r)$, between the ground state and excited state densities. $\Delta\rho(r)$ itself will have positive regions where electron density has increased during the transition ($\rho_+(r)$) and negative regions where it has diminished ($\rho_-(r)$). The difference between the barycenters of $\rho_+(r)$ and $\rho_-(r)$ is then referred to as D_{CT},[15] representing the distance over which charge transfer has occurred. This parameter is thus interpreted similarly to Δr, but is based on ground and excited state densities rather than linear combinations of orbital pairs. Note that a previous study has shown that D_{CT} and Δr (specifically a Δr variant based on natural transition orbitals[17]) correlate well with each other.[33]

D_{CT} does not account for how diffuse the electron density is for the ground or excited states or how this diffusivity could impact CT. This can be assessed by considering the RMSD of $\rho_{+/-}(r)$, referred to as $\sigma_{+/-}$, which measures the spread of the density changes. The density accumulation and depletion zones can be smoothed using $\sigma_{+/-}$, and these smoothed regions are referred to as $C_{+/-}(r)$.[15] Essentially, $C_{+/-}(r)$ can be thought of as more "averaged" versions of $\rho_{+/-}(r)$, which makes them simpler to interpret. Plots of $C_{+/-}(r)$ have been used previously to provide easier visualization of the overlap of density differences.[15] Here $C_{+/-}(r)$ is used quantitatively by measuring the overlap between $C_+(r)$ and $C_-(r)$ (referred to as S_C)[32] as shown below:

$$S_C = \int \sqrt{C_+(\mathbf{r})/A_+}\sqrt{C_-(\mathbf{r})/A_-}\, d\mathbf{r} \quad (1)$$

where $A_{+/-}$ are normalization constants. A larger S_C provides evidence of a local excitation whereas a smaller value indicates a charge transfer excitation. S_C can be thought of as a density analog to the orbital-based Λ described earlier. S_C has been proposed for use in the Multiwfn program (where

it is referred to as S_{+-}),[32] but we are not aware of any large-scale testing of its behavior in the literature. All of the CT parameters are shown in a qualitative fashion in Figure 2. Note that the descriptions given above are only meant to provide a simple physical interpretation of the parameters. Those looking for a more rigorous discussion should consult the original literature.[14-16] With the exception of Λ, all excited state parameters were calculated with Multiwfn version 3.4.[32] Λ was determined with a code developed in-house that was verified using data from Tozer's original paper.[14]

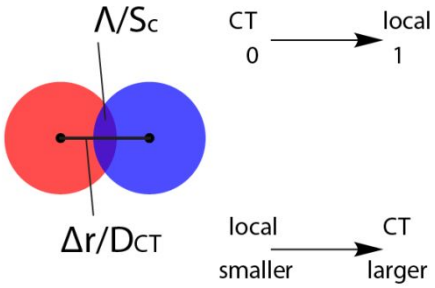

Figure 2. Qualitative cartoon illustrating CT parameters used in this study. For orbital-based parameters the red and blue circles represent φ_{ia} and for the density-based parameters they represent either $\rho_{+/-}(r)$ or $C_{+/-}(r)$ as appropriate.

Change in the Dipole Moment

The final CT parameter considered in this study is the change in the dipole moment between the ground and excited state, Δμ. This quantity is calculated as the difference between the ground and excited state dipole moments

$$\Delta\mu = \sqrt{(\mu_x^{ES} - \mu_x^{GS})^2 + (\mu_y^{ES} - \mu_y^{GS})^2 + (\mu_z^{ES} - \mu_z^{GS})^2} \quad (2)$$

where $(\mu_x^{GS}, \mu_y^{GS}, \mu_z^{GS})$ and $(\mu_x^{ES}, \mu_y^{ES}, \mu_z^{ES})$ represent the ground and excited state dipole moment vectors, respectively. A small change in the dipole moment corresponds to a local transition, while a large change in the moment indicates a CT excited state.[53-54]

Results and Discussion

Twenty organic dyes were obtained from the MWDL at NCSU (see Figure 1). The purity of all samples was verified by NMR spectroscopy and mass spectrometry (see Supporting Information for details). Having verified the purity of the samples, the experimentally measured

UV-Vis spectra were compared with the calculated ones. Note, that to our knowledge the experimental UV-Vis spectra of these dyes have never been reported before.

The rest of the manuscript is organized as follows: First, we describe the ground and excited state electronic structure of the dyes. We then summarize the results of our benchmarking studies and identify the functionals that provide the best description of the transitions in the visible region. Finally, we focus on understanding the relationship between the error in the calculated transition energies, the amount of exact exchange in the functional, and the CT character of the excited states of the dyes.

Ground state electronic structure

All dyes within each family share a common backbone (the highlighted components in Figure 1), and these parent dyes are referred to as **A0** and **C0** for the azo and cyano families, respectively. Therefore, it is useful to understand the electronic structure of **A0** and **C0** before analyzing the substituted dyes. Figure 3 shows the frontier orbitals of the parent dyes (calculated with B3LYP), along with the frontier orbitals of representative dyes from each family (**A3** and **C10**). The frontier orbitals of all other dyes are shown in the Supplemental Information. The HOMO of **A0** consists of π MOs (resembling the HOMO of benzene) on each aromatic ring interacting in an antibonding fashion with a N−N π bonding MO. The LUMO consists of π* MOs (resembling the LUMO of benzene) on each aromatic ring interacting in a bonding fashion with a N−N π* antibonding MO. A similar picture is seen for **C0**, except the aromatic MOs are now interacting with C−C π and π* MOs in the HOMO and LUMO, respectively. A strong resemblance of the HOMO and LUMO of the substituted dyes with the HOMO and LUMO of the parent dyes can clearly be seen. This resemblance is particularly strong for the LUMOs, while for the HOMOs of **A3** and **C10** there is little-to-no N−N or C−C (alkene) bonding character respectively, unlike what is seen for **A0** and **C0.**

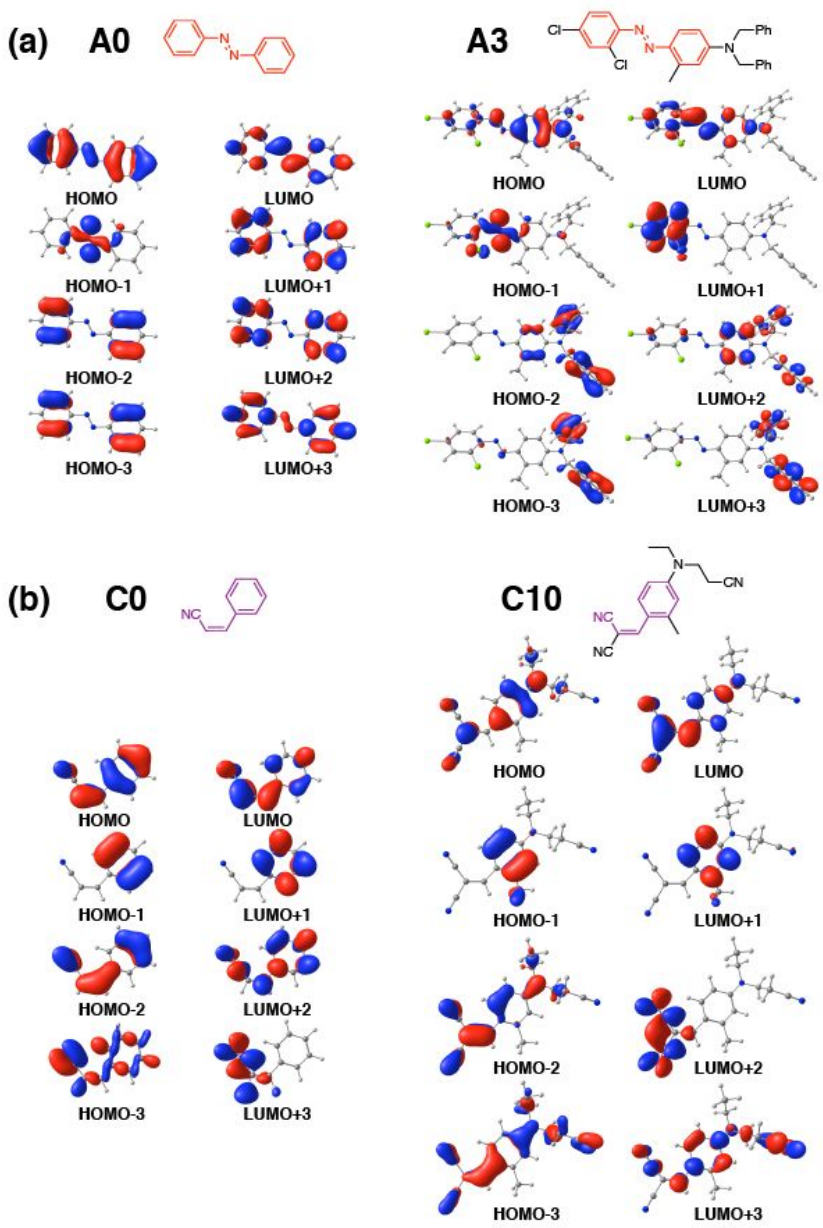

Figure 3. Frontier KS MOs for representative (a) azo dyes and (b) cyano dyes. All orbitals were calculated with the B3LYP functional.

General characterization of calculated transitions

Figure 4 shows the experimentally measured spectra of representative dyes from each family (**A3** and **C10**) and the calculated TD-DFT spectra with each of the functionals examined (all spectra are reported in the Supporting Information). The TD-DFT reasonably reproduces the qualitative shape of the UV-Vis spectra for each dye and changing the functional primarily shifts the energies of the calculated excitations. Generally, increasing the amount of HF_{Ex} causes a blue

shift of the spectra, as expected.[10, 29] Most of the dyes examined had in their experimental spectra one large, broad absorbance in the visible region (λ_{max}) and then varying amounts of high-energy transitions in the UV-region assignable as π-π* transitions. The visible transitions are of greatest interest for practical applications of dyes, and unless stated otherwise any further analysis will be on λ_{max} for all dyes.

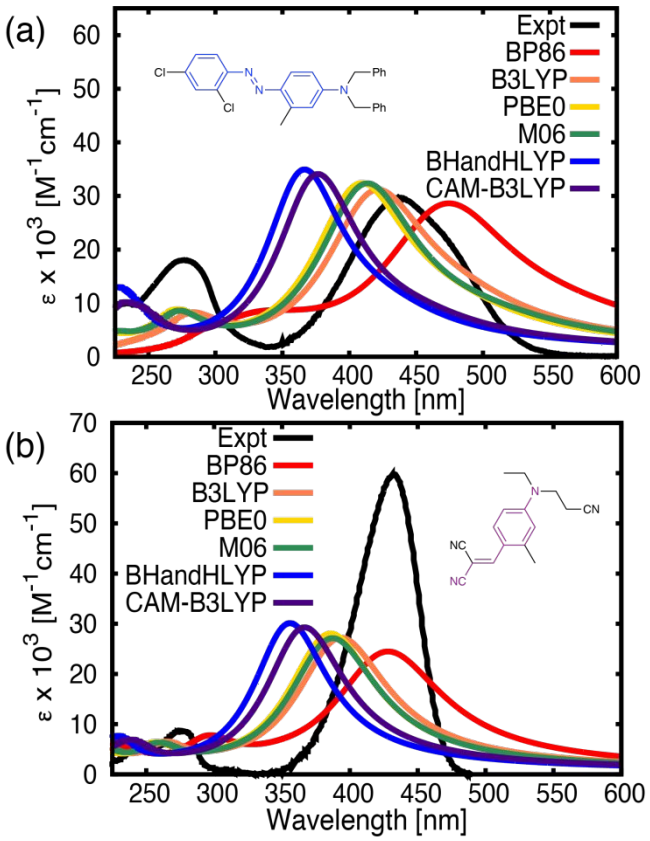

Figure 4. Experimentally measured and calculated TD-DFT spectra of (a) **A3** and (b) **C10**.

The dominant KS MOs involved in describing λ_{max} based on the TD-DFT transition densities are the HOMO and LUMO (although there are a few exceptions as discussed below), examples of which are shown in Figure 3. For both families, these transitions can then be qualitatively described as π-π*, HOMO to LUMO transitions. In the dyes investigated, there is also an amine attached to the aromatic ring. The "lone pair" MO of the amine is conjugated to the aromatic ring in an antibonding fashion in the HOMO, and to a lesser extent, the LUMO. This reflects how there is some CT from the amine group to either the azo or alkene moiety depending

on the dye family. These orbital shapes and assignments are essentially the same regardless of the methodology used in the calculation. Qualitatively similar MOs have also been noted in CT transitions of other organic dyes.[23]

Selection of λ_{max} from the TD-DFT results was straightforward for most of the dyes. For the azo dyes, the oscillator strength of the lowest energy transition was either zero or relatively small (less than 0.5), and can be assigned as an n-π^* transition from the azo nitrogen lone pairs into the N−N π^* orbital (this generally corresponds to the HOMO-1 to LUMO transition, see Figure 3). The second transition, the HOMO to LUMO transition described earlier, possesses much larger oscillator strength (0.62 to 1.41) and corresponds to λ_{max}. There are a few isolated cases (**A4**, **A5**, and **A7**) where the oscillator strength of the first transition is not completely negligible as mentioned above, but it is still much lower than the second transition, and hence the second transition was always chosen for λ_{max}.

For the cyano dyes, the lowest energy transition corresponding to the HOMO-LUMO transition displayed a wide range of oscillator strengths (from 0.09 to 1.08. The nitro-containing cyano dyes (**C3**, **C4**, and **C5**) possessed a second transition slightly more intense than the first transition and close in energy, making it difficult to tell which one (or if both) was responsible for the experimental λ_{max}. This second transition corresponds to the HOMO-LUMO+1 transition, where the LUMO+1 is an orbital of π^* character centered on the nitro group (see Supporting Information). Ultimately, the most intense transition was always chosen as λ_{max} whenever there was ambiguity for the cyano dyes. Note that the results do not change significantly with the other assignment and a brief analysis of the alternative assignments is provided in the SI.

Functional dependence of error

As can be expected based on the spread of the calculated spectra in Figure 3, some functionals match the experimental values of λ_{max} more accurately than others, and these results are summarized in Table 1 and Figure 5. Overall, the determined mean unsigned errors (MUEs) and mean signed errors (MSEs) were similar for each dye family. Note that error here is referred to as ΔE_{max} which is taken as E_{max}(calc) - E_{max}(expt), where E_{max} is simply λ_{max} reported in eV. For both the MSE and MUE, B3LYP, PBE0, and M06 yielded the smallest errors. All three of these functionals possess intermediate amounts of HF_{Ex} with 20%, 25%, and 27%, respectively. The one

GGA functional examined, BP86 (0% HF_{Ex}), did considerably worse than the hybrids, while BHandHLYP (50% HF_{Ex}) and the range-separated CAM-B3LYP (65% HF_{Ex} at large distances) had the overall worst errors. From an empirical standpoint, if the goal is simply to match λ_{max} as closely as possible, it is advisable for complexes similar to the dyes examined here to choose functionals with HF_{Ex} between 20-30%. These general recommendations are completely in line with conclusions that have been reached in other benchmarking studies on organic dyes.[10, 29] It has been suggested previously that the success of hybrid functionals with modest amounts of HF_{Ex} may be the result of the functional's inherent error and the LR solvation scheme's error cancelling each other out.[44] Although not evaluated here, one route to reducing the calculated errors in general is to employ the Tamm-Dancoff Approximation (TDA) as it has been shown to decrease errors associated with local excitations (i.e., excitations with a large Λ) that have triplet instability issues.[55] The excitations calculated in this study are, however, of "intermediate" CT character (see below), and it is not clear how effective the TDA would be. Exploring the impact of TDA is potentially worth considering in future studies on these systems.

ΔE_{max} is also plotted for each compound in Figure 5 which shows that BP86 virtually always redshifts calculated transitions relative to experiment, while CAM-B3LYP and BHandHLYP almost always blueshift relative to experiment; both of these trends are expected.[10, 29] The functionals with intermediate amounts of HF_{Ex} have varying signs of error (i.e., can both blueshift and redshift), but the errors are usually smaller than the errors of the other functionals. Note that **A1** appears to be an outlier amongst the azo dyes, as CAM-B3LYP and BHandHLYP are very accurate, while the excitation energies calculated with other functionals are more red-shifted than usual. This is possibly due to proton tautomerism on the triazole ring, which may occur rapidly in this system.[56-57] The calculations reported here are for the complex shown in Figure 1, as this was the complex as labeled in the MWDL. Calculations on the most relevant alternative tautomer of this structure, which is roughly isoenergetic, do show a blueshift of the spectra for each method by ~0.2 eV, bringing these results closer in line with the rest of the data. This data is described in more detail in the SI.

Table 1. MUEs and MSEs for calculation of ΔE_{max} for each dye family as determined with different functionals. All values are reported in eV.

MUE/MSE (eV)	BP86	B3LYP	PBE0	M06	BHandHLYP	CAM-B3LYP
Cyano	0.37/-0.36	0.17/0.07	0.23/0.17	0.22/0.17	0.61/0.61	0.51/0.51

Azo	0.35/-0.35	0.19/0.00	0.19/0.09	0.17/0.06	0.45/0.45	0.38/0.37

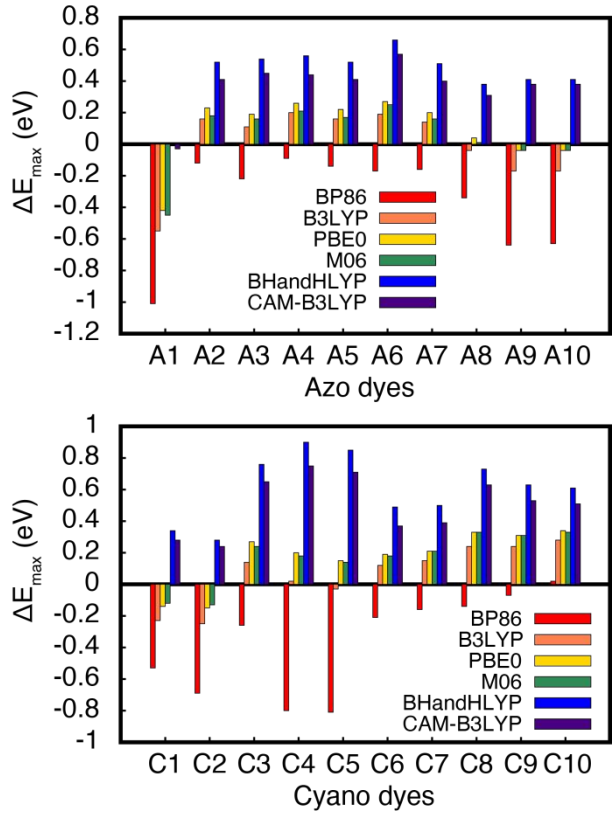

Figure 5. ΔE_{max} determined for all six functionals for both dye families.

The explicit relationship between ΔE_{max} and HF_{Ex} is shown more clearly in Figure 6 for each dye family. All the dyes show a similar, roughly linear dependence of ΔE_{max} on HF_{Ex}. Note that CAM-B3LYP was treated as if it had a constant HF_{Ex} value of 65%, when in reality this varies as a function of r_{12} and hence it deviates from the line. As the HF_{Ex} is increased, the error for all complexes changes from being negative (red shift) to positive (blue shift) as would be expected.[10, 29] This relationship between HF_{Ex} and error agrees with the results in Table 1 and Figure 5 for most compounds considered. Figure 6 again shows that intermediate values of HF_{Ex} display the smallest errors overall. Based on this data, it appears that while CAM-B3LYP and BHandHLYP have the advantage of showing the weakest dependence on CT as discussed below, their results have larger error. For the compounds considered, these are not the ideal functionals to choose for matching experiment.

Figure 7 shows the correspondence between the calculated values of E_{max} and the measured ones; if the calculated values were perfectly accurate then each of these plots would be exactly linear (R^2 = 1 for a linear fit) with a slope of 1. While the cyano dyes have reasonably good correlations (R^2 from 0.58 to 0.97), the azo dyes show much worse behavior (R^2 from 0 to 0.23). The difference in systematic behavior between the two dye families may be the result of the azo dyes spanning a smaller range of excitation values (~0.5 eV vs. ~1.5 eV), but the fact that the azo dyes do not show a strong systematic error over a 0.5 eV range is still troubling.

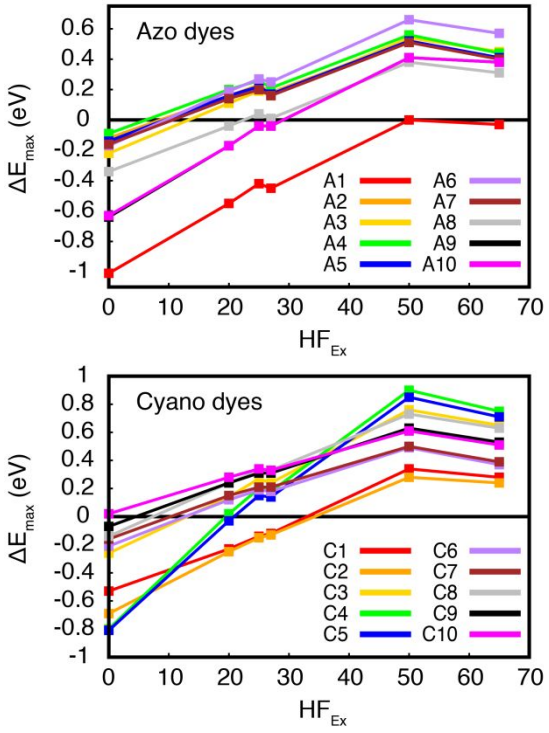

Figure 6. ΔE_{max} as a function of HF_{Ex} of the functional for each dye family.

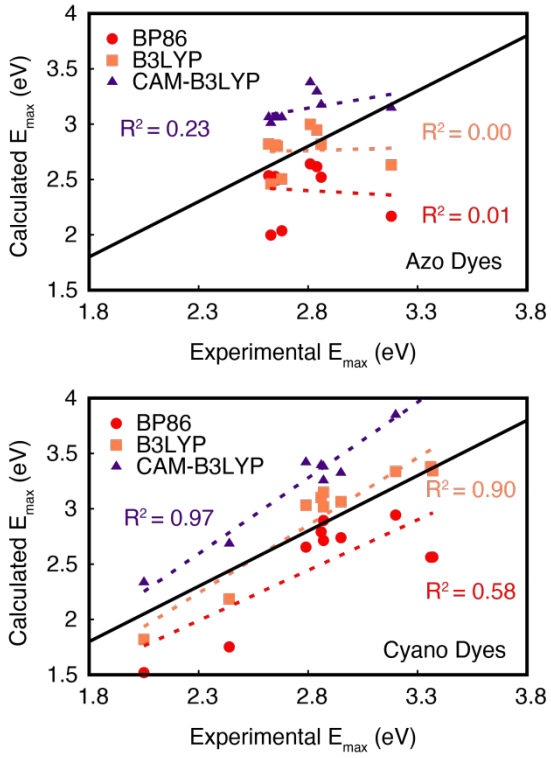

Figure 7. Relationship between calculated and experimental excitation energies (E_{max}) in each dye family. Note that only the data for three functionals (BP86, B3LYP, and CAM-B3LYP) are shown for simplicity.

Calculated HOMO-LUMO gaps and excitation energies

We have calculated HOMO-LUMO gaps for both series of dyes in order to evaluate whether the data that can be easily obtained from the ground state electronic structure calculations (such as orbital energies) could be employed to estimate the excitation energies for a large set of the dyes. Interestingly, the HOMO-LUMO gaps calculated with the B3LYP functional are within 0.3 eV of the experimental values for both dye families (see Table 2), with other functionals exhibiting substantial errors (0.5-2.6 eV), suggesting that B3LYP may be a good functional for fast preliminary screening of a large data set. High accuracy for HOMO-LUMO gaps has been seen for B3LYP in the past but was noted to likely be the result of fortuitous error cancellation,[58] suggesting that while the utility of the B3LYP results is encouraging, they should be interpreted cautiously. The plots of calculated HOMO-LUMO gaps vs. the measured E_{max} (shown in Figure 8) show essentially the same behavior as the plots of calculated E_{max} vs. the measured E_{max} (see Figure 7). The cyano dyes display very good correlations (R^2 from 0.75 to 0.92), while the azo dyes show no correlation (R^2 from 0 to 0.03). This indicates that calculated HOMO-LUMO gaps

may serve as a useful indicator for how accurate the calculated TD-DFT excitation energies will be in predicting trends for a particular set of dyes.

Table 2. MUEs and MSEs for calculation of ΔE_{max} for each dye family using HOMO-LUMO gap as determined with different functionals. All values are reported in eV.

MUE/MSE (eV)	BP86	B3LYP	PBE0	M06	BHandHLYP	CAM-B3LYP
Cyano	0.97/-0.97	0.29/0.27	0.58/0.58	0.73/0.73	2.28/2.28	2.62/2.62
Azo	0.99/-0.99	0.25/0.18	0.50/0.50	0.60/0.60	2.11/2.11	2.49/2.49

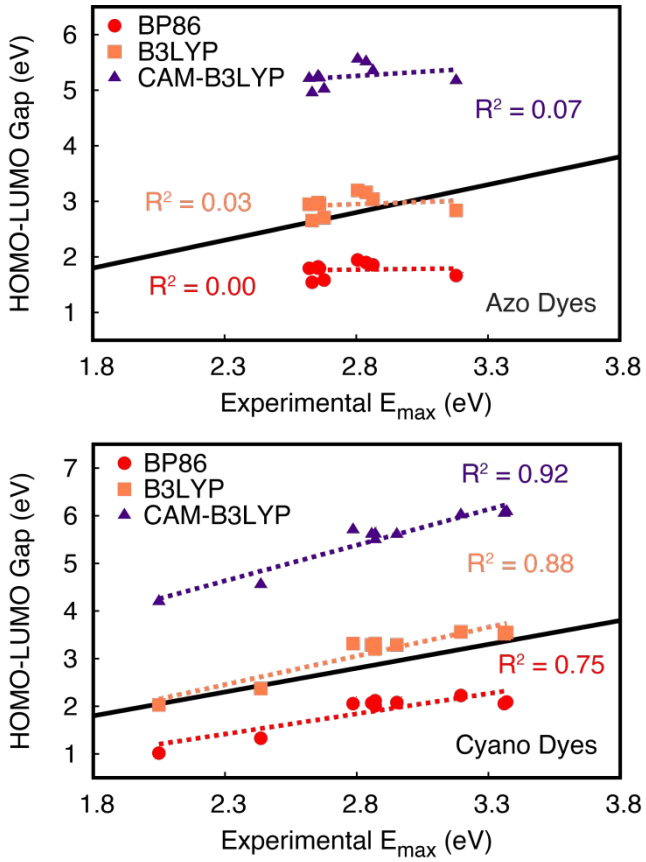

Figure 8. Relationship between calculated HOMO-LUMO gaps and experimental excitation energies (E_{max}) in each dye family. Note that only the data for three functionals (BP86, B3LYP, and CAM-B3LYP) are shown for simplicity.

Relationship between CT and functional dependence

It is well known that different DFT functionals have varying degrees of success when dealing with CT excitations.[10, 29] The key factor influencing this behavior is the amount of HF_{Ex}.

In this study, CAM-B3LYP and BHandHLYP incorporate a greater amount of HF_{Ex} and are therefore in theory better suited for handling CT excitations. Previous results studying CT transitions have shown that CAM-B3LYP showed no dependence of ΔE_{max} on CT, while hybrids showed modest dependence, and then pure functionals showed the greatest dependence.[14] This of course leads to the problematic issue of deciding whether the transitions investigated are in fact best classified as CT as opposed to local. As will be discussed below, the general conclusion reached here is that it is likely that the excitations under study have weak to moderate CT character, and hence the relationship between CT and ΔE_{max} may be more nuanced than for transitions with higher CT character.

A significant challenge for evaluating the connection between CT character and error is that there is not one "correct" method of measuring CT character. Although CT character can at times be qualitatively easy to recognize when viewing molecular orbitals, it is nontrivial to quantify. Many different parameters have been proposed to quantify it, but there is no universally accepted measure of CT. To account for this lack of an accepted parameter, five different methods were chosen to measure CT (see Figure 2), increasing the likelihood of being able to capture a correlation if it is present. Of the methods examined, Λ and Δr are both derived from analysis of calculated KS MOs, while D_{CT} and S_c are both calculated from ground and excited state densities. Finally, $\Delta\mu$ relies on comparison of ground and excited state dipole moments. As discussed earlier, to our knowledge, no large-scale evaluation on the behavior of S_c has been published previously. Orbital-based CT parameters are shown in Figure 9, density-based CT parameters are shown in Figure 10, and the $\Delta\mu$ parameter is shown in Figure 11.

Previously, Λ values between 0.1 to 0.8 have been associated with CT;[16] this large range, however, limits its discriminatory power. Based on this range, every λ_{max} transition examined here can be classified as a CT transition. Significant CT character was previously assumed if Δr was greater than 1.5 Å,[16] meaning λ_{max} for every cyano dye and every functional is classified as CT. The azo dyes show more variation in Δr; λ_{max} for **A1**, **A8**, **A9**, and **A10** dyes are all greater than 1.5 Å regardless of the functional and are therefore always classified as CT. The remaining azo dyes have Δr values much closer to the 1.5 Å cutoff, and are better classified as having an intermediate CT character. Note as well that for these dyes, because Δr is so close to the cutoff, results for a single λ_{max} transition from different functionals can provide Δr values above or below

the 1.5 Å cutoff. Thus, usage of different functionals for parameter measurement can change how a transition is actually classified (CT vs. local).

The density-based CT parameters shown in Figure 10 show similar trends overall as the orbital-based parameters, but the functional dependence in general appears to be more severe (especially note the variance in D_{CT} for **C4**, **C5**, **A1**, **A9**, and **A10**). Finally, the functional dependence of the Δμ parameter is shown as well in Figure 11. While several dyes show little variation in Δμ as the functional changes, several of the dyes fluctuate significantly (as for D_{CT} **C4**, **C5**, **A1**, **A9** and **A10**, but also **C1**, **C2**, and **C3**). Functional dependence of CT parameters (which has been reported previously[16]) can make it difficult to define clear cutoffs for when a transition is CT or local. In extreme cases (very high or very low CT character), this level of discrimination may not be that troublesome, but as can be seen for this data set, which includes numerous transitions of intermediate CT character, this spread can make differentiating CT from local transitions difficult. Furthermore, note that the benchmarking done in the literature so far has been on calculating the energy of a transition, and there is no rigorous reason to assume that a functional that can properly calculate λ_{max} will also be the best one for quantifying CT.

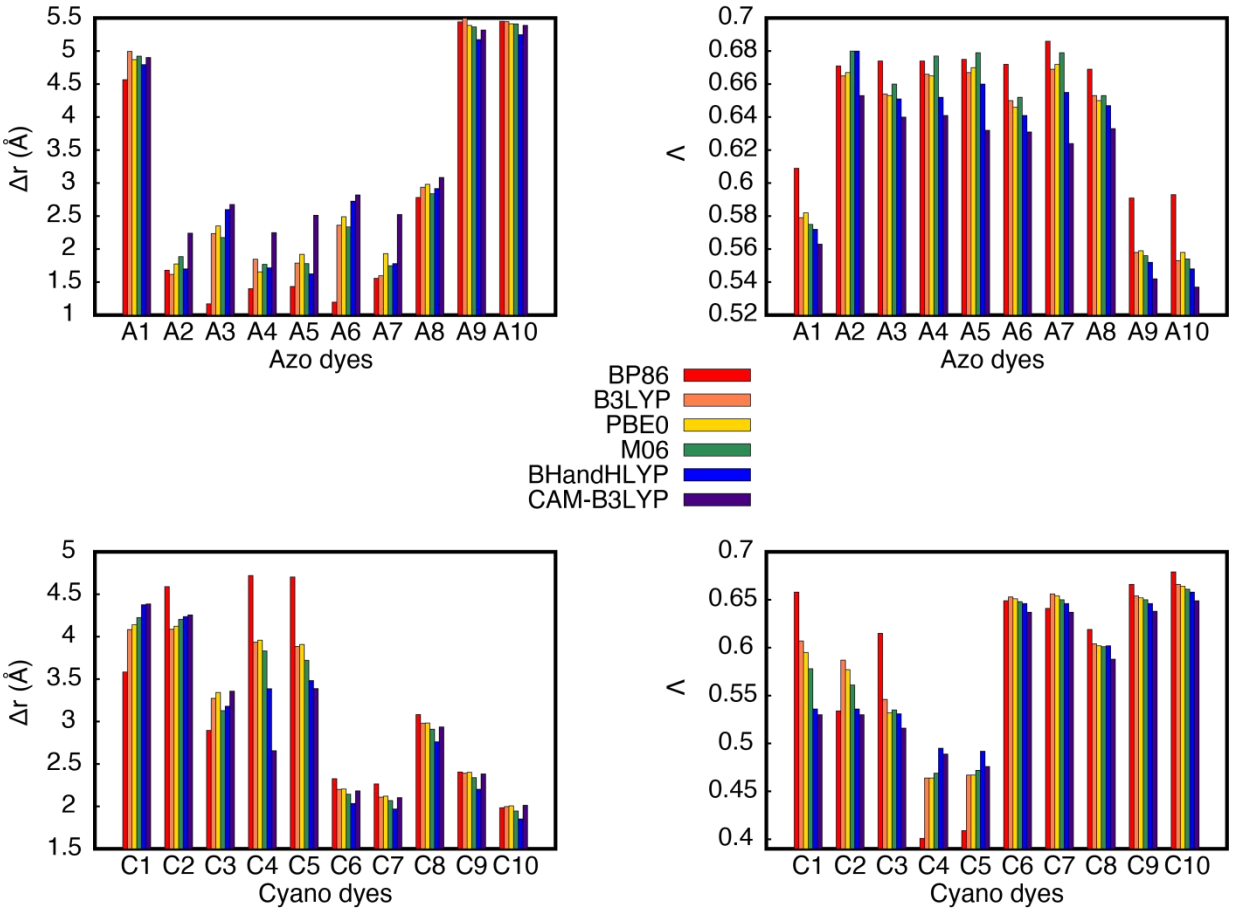

Figure 9. Calculated orbital-based CT parameters for both sets of dyes.

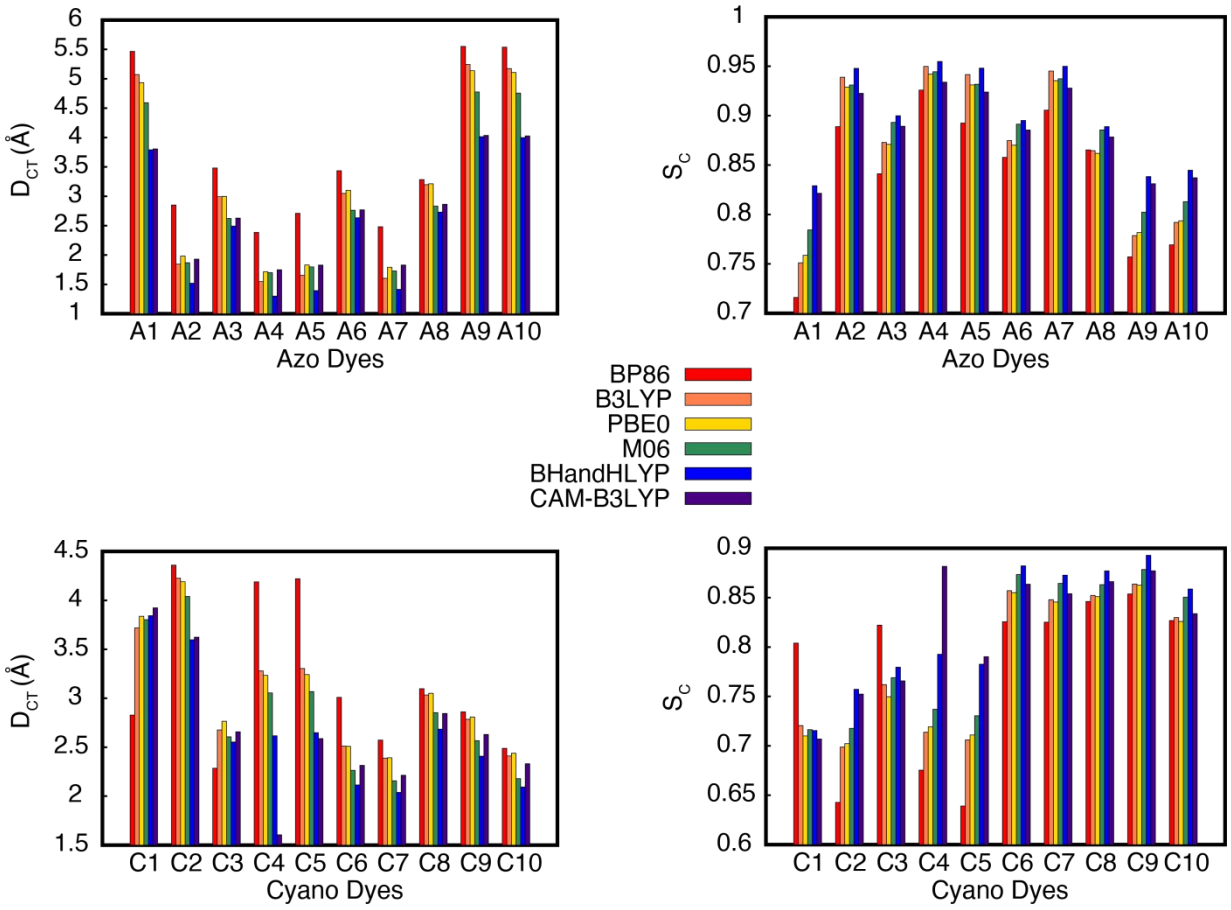

Figure 10. Calculated density-based CT parameters for both sets of dyes.

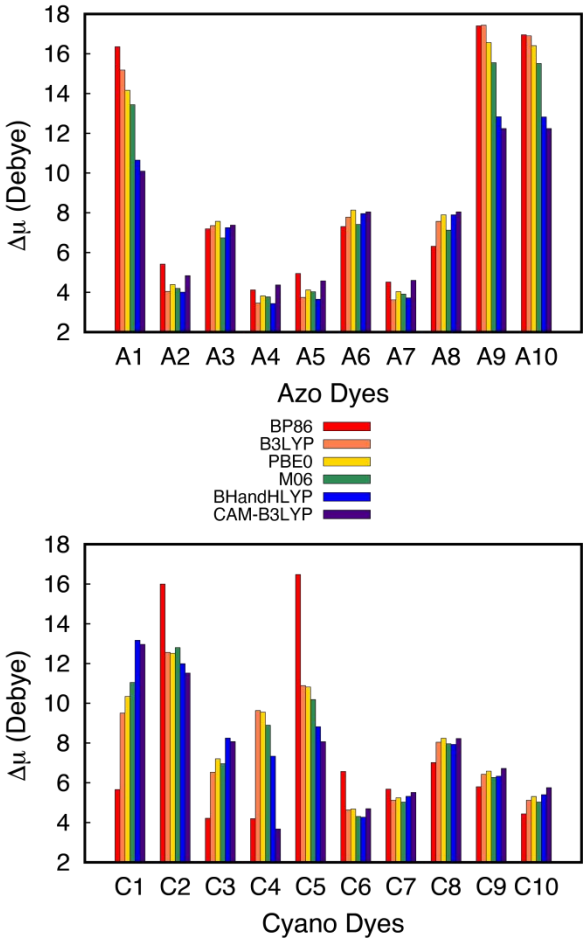

Figure 11. Calculated Δμ parameter for both sets of dyes.

To determine the relationship between CT character and functional accuracy, plots of ΔE_{max} vs. each CT parameter were generated (Figures 12 and 13 for Λ and Δr respectively; other plots are given in the SI). These figures show that for the azo family the amount of HF_{Ex} present in the functional has a clear effect on the degree to which ΔE_{max} can be predicted from CT character. The lower the HF_{Ex} (recall that it is 0 for BP86), the stronger the dependence of ΔE_{max} on CT character. The cyano dye family shows the same behavior for Δr, but the impact of functional is not as clear for the relationship between ΔE_{max} and Λ; BP86 still shows a high correlation for both parameters, but CAM-B3LYP and B3LYP both show the same weak correlation despite having very different HF_{Ex} (65% and 20% respectively).

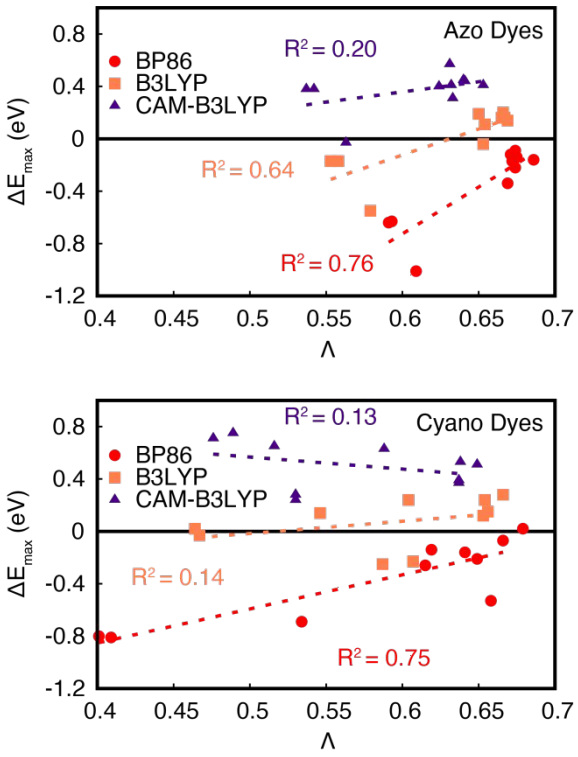

Figure 12. Relationship between Λ and ΔE_{max}. Note that only three functionals are shown for brevity.

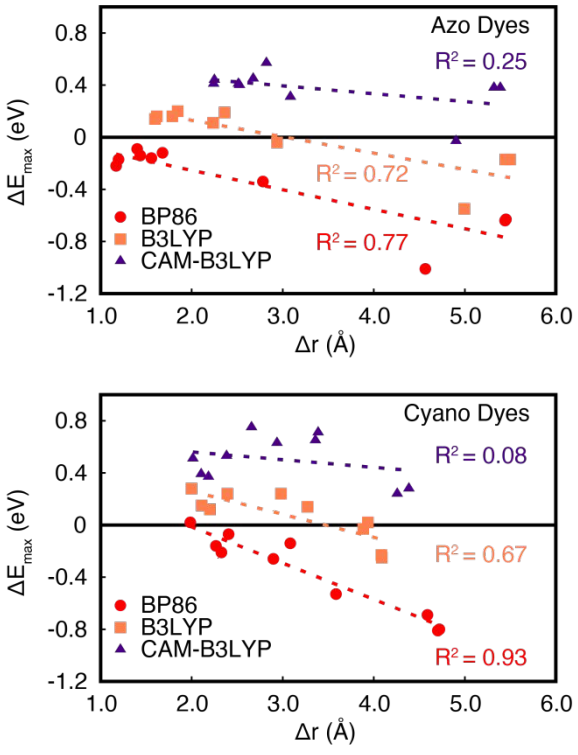

Figure 13. Relationship between Δr and ΔE_{max}. Note that only three functionals are shown for brevity.

To visualize this behavior more clearly for the entire data set (all CT parameters and all functionals), several heat maps were generated based on the R^2 values for plots similar to Figures 12 and 13 (see Figure 14). The x-axis in these plots indicates the functionals used, while the y-axis indicates which CT parameter is being correlated against ΔE_{max}. Each square was then colored based on the magnitude of R^2, where the darker/warmer colors signify larger calculated values of R^2 and therefore a stronger dependence of ΔE_{max} on CT. If the HF_{Ex} dependence of ΔE_{max} was equally well predicted by each CT parameter and was similar to what Tozer had reported previously for Λ,[14] then the heat map should be very dark on the left side of the plot (low HF_{Ex}) and become increasingly light on moving to the right side of the plot (high HF_{Ex}).

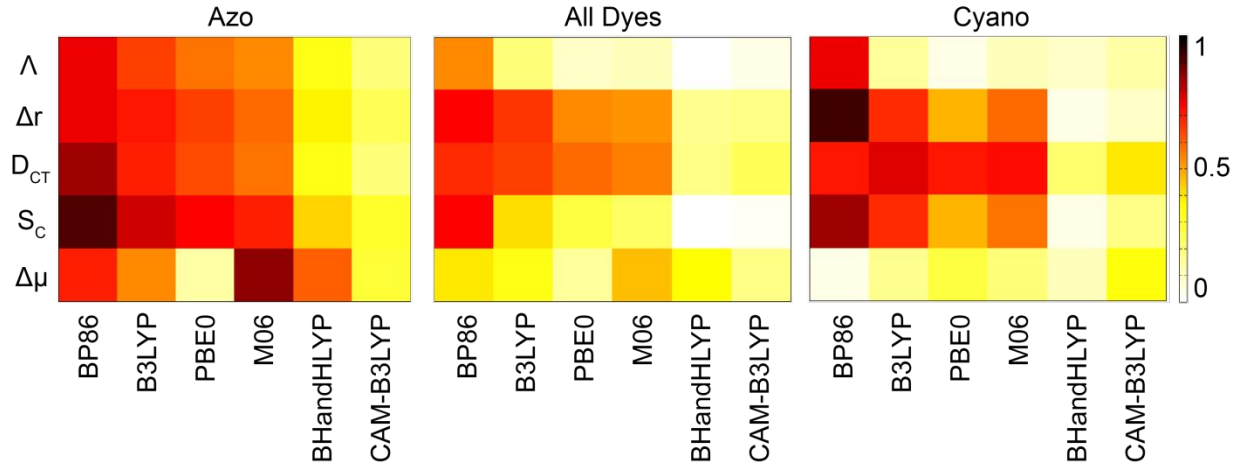

Figure 14. Heat maps showing R^2 for the correlation of each CT parameter with ΔE_{max}.

From the coloring of the maps, it is clear that several CT parameters in each dye family obey this relationship, but that this behavior is not always consistent between the two families. For the cyano family, the relationship between ΔE_{max} and Λ as well as $\Delta\mu$ shows no consistent dependence on the amount of HF_{Ex} in the functional (as expected based on Figure 12), but there is a clear relationship with Δr, D_{CT}, and S_C. The azo family also shows strong relationships with all CT parameters, with the exception of $\Delta\mu$. Specifics aside, the truly critical observation to draw from these results is that the two dye families do not exhibit the same types of relationships between ΔE_{max}, HF_{Ex}, and CT. This is evident when all of the dyes are taken together as one dataset. Only the distance-based (Δr and D_{CT}) parameters show consistent functional dependence for both sets of dyes, a result which is consistent with previous work that showed that Δr and D_{CT} generally

correlate well with each other.[33] The fact that Λ and Δr behaved similar in one dataset but not the other may also be consistent with previous work that showed that while the two parameters generally complement each other, Λ has weaker CT discriminating ability and occasionally failed in challenging cases.[16] Particularly interesting is that S_c showed the expected functional dependence for each family separately, but this relationship is significantly lessened for the entire dataset. Therefore, while the distance-based parameters certainly appear to have a more predictable relationship between error and functional choice, it is entirely possible that addition of another family of dyes would change this conclusion. Different functional dependence for dyes of different molecular sizes[29] has been reported previously. To our knowledge however, different functional dependence for different dye families and a molecular family-specific relationship between CT, error, and functional has not been discussed before, and should be considered when evaluating functional behavior.

Note we also explored the possibility that the erratic and confusing correlations between error and CT need to make use of multivariable linear regression. This idea was examined using LASSO analysis (see SI for discussion) but it did not result in significantly different conclusions. Another possible explanation is that the present set of molecules is too small to make strong conclusions. We are currently addressing this by analyzing more dyes from the MWDL, but if that is truly the case, then it does not bode well for CT being a useful diagnostic for functional dependence as practical computational studies will not always have access to massive sets of data. Overall, the results of the CT analysis show that the relationship between ΔE_{max}, HF_{Ex} and CT is not straightforward. These relationships may be particularly ambiguous when dealing with excitations with only moderate CT character. It is still likely that CT can serve as a useful tool for functional choice as seen with Δr and D_{CT} here, but it should be approached cautiously and with the understanding that the quantification of CT character and its significance may vary considerably between different molecular families.

One final point to be addressed is the choice of solvent polarization scheme for the TD-DFT calculations. As discussed in the methodology section, all the data presented thus far used the typical LR scheme, although SS solvation has been recommended for handling CT transitions, particularly with range-separated hybrid functionals such as CAM-B3LYP.[44] As the dyes analyzed here exhibited moderate CT character it was not clear how SS solvation would change the results. To gauge this, ΔE_{max} was calculated using the IBSF SS polarization scheme, and the MUE and

MSE are reported in Table 3. A technical issue that must be addressed was that in several instances applying SS corrections would change the nature of the excited state that was converged upon; essentially picking a different root than was originally specified in the LR calculation. This made it impossible to have a consistent comparison between the IBSF and LR data for every dye and functional. Fortunately, these problems only occurred for several BP86 calculations, and also for the dyes **C3**, **C4**, and **C5** (all functionals), so this data was then omitted for determining the effect of SS solvation corrections (discussed in SI).

The data in Table 3 show that application of the IBSF scheme offered mild improvement for the ΔE_{max} obtained from CAM-B3LYP (as expected) and BHandHLYP calculations; reducing their MUE by 0.11 eV for the cyano dyes and 0.03 eV for the azo dyes. Note, that these functionals still perform poorly compared to the other hybrid functionals, even with this improvement. For all other functionals, the IBSF method only increased the error, sometimes considerably so in the case of the azo dyes. Given the generally underwhelming effect of the IBSF corrections, an in-depth analysis of the IBSF-calculated CT parameters was not conducted. However, some discussion of this issue is provided in the SI. There are other SS solvation schemes available,[59-60] and it may prove interesting in future work to see how the chosen solvent polarization scheme affects calculated CT parameters.

Finally, another promising avenue of functional and solvation model optimization for TDDFT is the use of screened range separated hybrid functionals in tandem with PCM models (SRSH-PCM). A recent study showed significant error reduction in the characterization of CT transitions using SRSH-PCM in comparison to standard RSH functionals.[61] In future work we plan to evaluate the SRSH-PCM model on our test set of "intermediate" CT transitions, along with the optimally-tuned functionals mentioned in the introduction, to see if they show error dependence on CT parameters as the "standard" functionals evaluated here.

Table 3. MUEs and MSEs for calculation of ΔE_{max} for each dye family as determined with different functionals using the LR and IBSF SS solvent polarization schemes. Data for BP86 and dyes **C3**, **C4**, and **C5** have been omitted (see text). All values are reported in eV.

MUE/MSE (eV)	Solvation scheme	B3LYP	PBE0	M06	BHandHLYP	CAM-B3LYP
Cyano	IBSF	0.24/-0.04	0.26/0.04	0.27/0.05	0.40/0.40	0.31/0.31

Azo	LR	0.22/0.08	0.24/0.15	0.23/0.16	0.51/0.51	0.42/0.42
	IBSF	0.32/-0.12	0.31/-0.02	0.29/-0.03	0.42/0.39	0.35/0.31
	LR	0.19/0.00	0.19/0.09	0.17/0.06	0.45/0.45	0.38/0.37

Conclusions

Twenty compounds were selected essentially at random from the MWDL and their experimental and computational characterization was used to draw new insights about the impact of CT on error in TD-DFT and its dependence on molecular family. The MWDL was shown to be an excellent source of interesting organic dyes for TD-DFT benchmarking, and the results obtained from this work will be useful for further characterization of similar azo and cyano dyes from the library. It was conclusively demonstrated that functionals with intermediate HF_{Ex} (20-30%) are the most accurate for matching the experimentally determined values of λ_{max} for all of the dyes examined. Interestingly enough, CAM-B3LYP was found to be very poor at matching experimental values, although it did show very little dependence of its error on CT character. It is also important to note that while the cyano dye family exhibited systematic error in calculated E_{max} for most of the DFT functionals examined, the error in calculated E_{max} for dyes in the azo family was not systematic for any of the functionals examined. This illustrates the difficulty in utilizing TD-DFT even for predicting qualitative trends in excitation energies in certain dye families and in extrapolating usefulness of a particular functional from one dye family to another. Interestingly, calculated HOMO-LUMO gaps were found to be a useful predictor for the accuracy of the calculated TD-DFT excitation energies.

Beyond being able to generally recommend what functionals are useful for these types of dyes, the present work also explored the relationship between CT and a given functional's accuracy in matching the experimental λ_{max}. This study compared three popular CT quantification methods (Λ, Δr, and D_{CT}) simultaneously on the same dataset and also included the previously untested S_C parameter along with the dipole-based parameter $\Delta\mu$. There was a strong dependence of λ_{max} on HF_{Ex} for each dye family, but the actual errors were not systematic across the two molecular families, which can make qualitative and quantitative comparison of the dyes across different families difficult. It was found that while Δr and D_{CT} demonstrated a consistent relationship between ΔE_{max} and the amount of HF_{Ex} in the DFT functional for both dye families, no other CT

parameter was equally reliable. While Λ and S_C parameters have shown some systematic behavior, it was only within specific families of dyes. Finally, the Δμ parameter did not exhibit systematic behavior in any of the dye families. This study has provided evidence that the relationship between the CT character of a transition and ΔE_{max} is not necessarily straightforward, and that the origin of functional dependence of TD-DFT calculations on organic dyes is complex and requires careful choices on how to quantify CT character.

Supporting Information

Molecular orbitals of all dyes, calculated and experimental UV-Vis spectra, LASSO analysis, NMR and LC-MS characterization details. A data file containing xyz coordinates of all dye structures optimized at the B3LYP+D2/6-311G* level of theory.

Author Information

Corresponding Author

*E-mail: ejakubi@ncsu.edu

Notes

The authors declare no competing financial interest.

Acknowledgments

This work was supported by the National Science Foundation grant CHE-1554855. NRV gratefully thanks the NC State Chancellor's Faculty Excellence Program. RDM acknowledges the support and training of the Blue Waters Student Internship Program. This research is part of the Blue Waters sustained-petascale computing project, which is supported by the National Science Foundation (awards OCI-0725070 and ACI-1238993) and the state of Illinois. Blue Waters is a joint effort of the University of Illinois at Urbana-Champaign and its National Center for Supercomputing Applications.

References

1. M. J. Melo, History of Natural Dyes in the Ancient Mediterranean World. *Handbook of Natural Colorants* 2009, 1.

2. J. V. Goodpaster; E. A. Liszewski, Forensic Analysis of Dyed Textile Fibers. *Anal. Bioanal. Chem.* 2009, **394**, 2009.

3. M. A. Kuenemann; M. Szymczyk; Y. Chen; N. Sultana; D. Hinks; H. S. Freeman; A. J. Williams; D. Fourches; N. R. Vinueza, Weaver's Historic Accessible Collection of Synthetic Dyes: A Cheminformatics Analysis. *Chem. Sci.* 2017, **8**, 4334.

4. L. Gonzalez; D. Escudero; L. Serrano-Andres, Progress and Challenges in the Calculation of Electronic Excited States. *Chem. Phys. Chem.* 2012, **13**, 28.

5. A. D. Laurent; C. Adamo; D. Jacquemin, Dye Chemistry with Time-Dependent Density Functional Theory. *Phys. Chem. Chem. Phys.* 2014, **16**, 14334.

6. K. Burke, Perspective on Density Functional Theory. *J. Chem. Phys.* 2012, **136**, 150901.

7. E. Runge; E. K. U. Gross, Density-Functional Theory for Time-Dependent Systems. *Phys. Rev. Lett.* 1984, **52**, 997.

8. M. E. Casida, Time-Dependent Density Functional Response Theory for Molecules. In *Recent Advances in Density Functional Methods*, WORLD SCIENTIFIC: 1995; Vol. Volume 1, pp 155.

9. C. Adamo; D. Jacquemin, The Calculations of Excited-State Properties with Time-Dependent Density Functional Theory. *Chem. Soc. Rev.* 2013, **42**, 845.

10. A. D. Laurent; D. Jacquemin, TD-DFT Benchmarks: A Review. *Int. J. Quantum Chem.* 2013, **113**, 2019.

11. A. Natansohn; P. Rochon, Photoinduced Motions in Azo-Containing Polymers. *Chem. Rev.* 2002, **102**, 4139.

12. D. Jacquemin; E. A. Perpète; G. E. Scuseria; I. Ciofini; C. Adamo, Td-Dft Performance for the Visible Absorption Spectra of Organic Dyes: Conventional Versus Long-Range Hybrids. *J. Chem. Theory Comput.* 2008, **4**, 123.

13. J. Calbo, Optical Properties of DMA-π-DCV Derivatives: A Theoretical Inspection under the Dft Microscope. *J. Spectrosc.* 2016, **2016**, 1.

14. M. J. Peach; P. Benfield; T. Helgaker; D. J. Tozer, Excitation Energies in Density Functional Theory: An Evaluation and a Diagnostic Test. *J. Chem. Phys.* 2008, **128**, 044118.

15. T. Le Bahers; C. Adamo; I. Ciofini, A Qualitative Index of Spatial Extent in Charge-Transfer Excitations. *J. Chem. Theory Comput.* 2011, **7**, 2498.

16. C. A. Guido; P. Cortona; B. Mennucci; C. Adamo, On the Metric of Charge Transfer Molecular Excitations: A Simple Chemical Descriptor. *J. Chem. Theory Comput.* 2013, **9**, 3118.

17. C. A. Guido; P. Cortona; C. Adamo, Effective Electron Displacements: A Tool for Time-Dependent Density Functional Theory Computational Spectroscopy. *J. Chem. Phys.* 2014, **140**, 104101.

18. M. J. G. Peach; D. J. Tozer, Illustration of a Tddft Spatial Overlap Diagnostic by Basis Function Exponent Scaling. *THEOCHEM* 2009, **914**, 110.

19. M. J. G. Peach; C. R. L. Sueur; K. Ruud; M. Guillaume; D. J. Tozer, Tddft Diagnostic Testing and Functional Assessment for Triazene Chromophores. *Phys. Chem. Chem. Phys.* 2009, **11**, 4465.

20. K. A. Nguyen; P. N. Day; R. Pachter, The Performance and Relationship among Range-Separated Schemes for Density Functional Theory. *J. Chem. Phys.* 2011, **135**, 074109.

21. H. Nitta; I. Kawata, A Close Inspection of the Charge-Transfer Excitation by Tddft with Various Functionals: An Application of Orbital- and Density-Based Analyses. *Chem. Phys.* 2012, **405**, 93.

22. Y. Zhao; D. G. Truhlar, Density Functional for Spectroscopy: No Long-Range Self-Interaction Error, Good Performance for Rydberg and Charge-Transfer States, and Better Performance on Average Than B3lyp for Ground States. *J. Phys. Chem. A* 2006, **110**, 13126.

23. P. Dev; S. Agrawal; N. J. English, Determining the Appropriate Exchange-Correlation Functional for Time-Dependent Density Functional Theory Studies of Charge-Transfer Excitations in Organic Dyes. *J. Chem. Phys.* 2012, **136**, 224301.

24. D. Jacquemin; B. Moore; A. Planchat; C. Adamo; J. Autschbach, Performance of an Optimally Tuned Range-Separated Hybrid Functional for 0–0 Electronic Excitation Energies. *J. Chem. Theory Comput.* 2014, **10**, 1677.

25. A. Karolewski; T. Stein; R. Baer; S. Kümmel, Communication: Tailoring the Optical Gap in Light-Harvesting Molecules. *J. Chem. Phys.* 2011, **134**, 151101.

26. S. Kümmel, Charge-Transfer Excitations: A Challenge for Time-Dependent Density Functional Theory That Has Been Met. *Adv. Energy Mater.* 2017, **7**, 1700440.

27. T. Stein; L. Kronik; R. Baer, Prediction of Charge-Transfer Excitations in Coumarin-Based Dyes Using a Range-Separated Functional Tuned from First Principles. *J. Chem. Phys.* 2009, **131**, 244119.

28. A. Karolewski; L. Kronik; S. Kümmel, Using Optimally Tuned Range Separated Hybrid Functionals in Ground-State Calculations: Consequences and Caveats. *J. Chem. Phys.* 2013, **138**, 204115.

29. D. Jacquemin; V. Wathelet; E. A. Perpète; C. Adamo, Extensive Td-Dft Benchmark: Singlet-Excited States of Organic Molecules. *J. Chem. Theory Comput.* 2009, **5**, 2420.

30. S. S. Leang; F. Zahariev; M. S. Gordon, Benchmarking the Performance of Time-Dependent Density Functional Methods. *J. Chem. Phys.* 2012, **136**, 104101.

31. J. Tao; S. Tretiak; J.-X. Zhu, Performance of a Nonempirical Meta–Generalized Gradient Approximation Density Functional for Excitation Energies. *J. Chem. Phys.* 2008, **128**, 084110.

32. L. Tian; C. Feiwu, Multiwfn: A Multifunctional Wavefunction Analyzer. *J. Comp. Chem.* 2012, **33**, 580.

33. M. Savarese; C. A. Guido; E. Brémond; I. Ciofini; C. Adamo, Metrics for Molecular Electronic Excitations: A Comparison between Orbital- and Density-Based Descriptors. *J. Phys. Chem. A* 2017, **121**, 7543.

34. T. Yanai; D. P. Tew; N. C. Handy, A New Hybrid Exchange–Correlation Functional Using the Coulomb-Attenuating Method (Cam-B3lyp). *Chem. Phys. Lett.* 2004, **393**, 51.

35. A. D. Becke, Density-Functional Exchange-Energy Approximation with Correct Asymptotic Behavior. *Phys. Rev. A* 1988, **38**, 3098.

36. A. D. Becke, Density-Functional Thermochemistry. III. The Role of Exact Exchange. *J. Chem. Phys.* 1993, **98**, 5648.

37. A. D. Becke, A New Mixing of Hartree–Fock and Local Density-Functional Theories. *J. Chem. Phys.* 1993, **98**, 1372.

38. C. Lee; W. Yang; R. G. Parr, Development of the Colle-Salvetti Correlation-Energy Formula into a Functional of the Electron Density. *Phys. Rev. B* 1988, **37**, 785.

39. S. Grimme, Semiempirical Gga-Type Density Functional Constructed with a Long-Range Dispersion Correction. *J. Comp. Chem.* 2006, **27**, 1787.

40. R. Krishnan; J. S. Binkley; R. Seeger; J. A. Pople, Self-Consistent Molecular Orbital Methods. Xx. A Basis Set for Correlated Wave Functions. *J. Chem. Phys.* 1980, **72**, 650.

41. S. Miertuš; E. Scrocco; J. Tomasi, Electrostatic Interaction of a Solute with a Continuum. A Direct Utilization of Ab Initio Molecular Potentials for the Prevision of Solvent Effects. *Chem. Phys.* 1981, **55**, 117.

42. S. Miertuš; J. Tomasi, Approximate Evaluations of the Electrostatic Free Energy and Internal Energy Changes in Solution Processes. *Chem. Phys.* 1982, **65**, 239.

43. J. L. Pascual-ahuir; E. Silla; I. Tuñon, Gepol: An Improved Description of Molecular Surfaces. Iii. A New Algorithm for the Computation of a Solvent-Excluding Surface. *J. Comp. Chem.* 1994, **15**, 1127.

44. C. A. Guido; D. Jacquemin; C. Adamo; B. Mennucci, Electronic Excitations in Solution: The Interplay between State Specific Approaches and a Time-Dependent Density Functional Theory Description. *J. Chem. Theory Comput.* 2015, **11**, 5782.

45. R. Improta; V. Barone; G. Scalmani; M. J. Frisch, A State-Specific Polarizable Continuum Model Time Dependent Density Functional Theory Method for Excited State Calculations in Solution. *J. Chem. Phys.* 2006, **125**, 054103.

46. J. P. Perdew, Density-Functional Approximation for the Correlation Energy of the Inhomogeneous Electron Gas. *Phys. Rev. B* 1986, **33**, 8822.

47. J. P. Perdew; K. Burke; M. Ernzerhof, Generalized Gradient Approximation Made Simple. *Phys. Rev. Lett.* 1996, **77**, 3865.

48. J. P. Perdew; K. Burke; M. Ernzerhof, Generalized Gradient Approximation Made Simple [Phys. Rev. Lett. 77, 3865 (1996)]. *Phys. Rev. Lett.* 1997, **78**, 1396.

49. C. Adamo; V. Barone, Toward Reliable Density Functional Methods without Adjustable Parameters: The PBE0 Model. *J. Chem. Phys.* 1999, **110**, 6158.

50. M. Ernzerhof; G. E. Scuseria, Assessment of the Perdew–Burke–Ernzerhof Exchange-Correlation Functional. *J. Chem. Phys.* 1999, **110**, 5029.

51. Y. Zhao; D. G. Truhlar, The M06 Suite of Density Functionals for Main Group Thermochemistry, Thermochemical Kinetics, Noncovalent Interactions, Excited States, and Transition Elements: Two New Functionals and Systematic Testing of Four M06-Class Functionals and 12 Other Functionals. *Theor. Chem. Acc.* 2008, **120**, 215.

52. M. J. Frisch; G. W. Trucks; H. B. Schlegel; G. E. Scuseria; M. A. Robb; J. R. Cheeseman; G. Scalmani; V. Barone; B. Mennucci; G. A. Petersson; H. Nakatsuji; M. Caricato; X. Li; H. P. Hratchian; A. F. Izmaylov; J. Bloino; G. Zheng; J. L. Sonnenberg; M. Hada; M. Ehara; K. Toyota; R. Fukuda; J. Hasegawa; M. Ishida; T. Nakajima; Y. Honda; O. Kitao; H. Nakai; T. Vreven; J. A. Montgomery, Jr.; J. E. Peralta; F. Ogliaro; M. Bearpark; J. J. Heyd; E. Brothers; K. N. Kudin; V. N. Staroverov; R. Kobayashi; J. Normand; K. Raghavachari; A. Rendell; J. C. Burant; S. S. lyengar; J. Tomasi; M. Cossi; N. Rega; N. J. Millam; M. Klene; J. E. Knox; J. B. Cross; V. Bakken; C. Adamo; J. Jaramillo; R. Gomperts; R. E. Stratmann; O. Yazyev; A. J. Austin; R. Cammi; C. Pomelli; J. W. Ochterski; R. L. Martin; K. Morokuma; V. G. Zakrzewski; G. A. Voth; P. Salvador;

J. J. Dannenberg; S. Dapprich; A. D. Daniels; Ö. Farkas; J. B. Foresman; J. V. Ortiz; J. Cioslowski; D. J. Fox *Gaussian 09, Rev D.01*, Gaussian, Inc.: Willingford CT, 2009.

53. D. Jacquemin, Excited-State Dipole and Quadrupole Moments: TD-DFT Versus CC2. *J. Chem. Theory Comput.* 2016, **12**, 3993.

54. S. I. Lu; L. T. Gao, Calculations of Electronic Excitation Energies and Excess Electric Dipole Moments of Solvated P-Nitroaniline with the EOM-CCSD-PCM Method. *J. Phys. Chem. A* 2018, **122**, 6062.

55. M. J. G. Peach; D. J. Tozer, Overcoming Low Orbital Overlap and Triplet Instability Problems in Tddft. *J. Phys. Chem. A* 2012, **116**, 9783.

56. A. V. Dolzhenko; G. Pastorin; A. V. Dolzhenko; W. K. Chui, An Aqueous Medium Synthesis and Tautomerism Study of 3(5)-Amino-1,2,4-Triazoles. *Tetrahedron Lett.* 2009, **50**, 2124.

57. W. P. Ozimiński; J. C. Dobrowolski; A. P. Mazurek, DFT Studies on Tautomerism of C5-Substituted 1,2,4-Triazoles. *THEOCHEM* 2004, **680**, 107.

58. U. Salzner; J. B. Lagowski; P. G. Pickup; R. A. Poirier, Design of Low Band Gap Polymers Employing Density Functional Theory—Hybrid Functionals Ameliorate Band Gap Problem. *J. Comp. Chem.* 1997, **18**, 1943.

59. M. Caricato; B. Mennucci; J. Tomasi; F. Ingrosso; R. Cammi; S. Corni; G. Scalmani, Formation and Relaxation of Excited States in Solution: A New Time Dependent Polarizable Continuum Model Based on Time Dependent Density Functional Theory. *J. Chem. Phys.* 2006, **124**, 124520.

60. A. V. Marenich; C. J. Cramer; D. G. Truhlar; C. A. Guido; B. Mennucci; G. Scalmani; M. J. Frisch, Practical Computation of Electronic Excitation in Solution: Vertical Excitation Model. *Chem. Sci.* 2011, **2**, 2143.

61. S. Bhandari; B. D. Dunietz, Quantitative Accuracy in Calculating Charge Transfer State Energies in Solvated Molecular Complexes Using a Screened Range Separated Hybrid Functional within a Polarized Continuum Model. *J. Chem. Theory Comput.* 2019, **15**, 4305.